

Dynamics of Firing Patterns in Evolvable Hierarchically Organized Neural Networks

Olga Chibirova¹, Javier Iglesias^{1,2}, Vladyslav Shaposhnyk¹,
and Alessandro E.P. Villa¹

¹ Grenoble Institut des Neurosciences-GIN, INSERM UMRS 836,
NeuroHeuristic Research Group Université Joseph Fourier, Grenoble 1, France
{Olga.Chibirova,Javier.Iglesias,Vladyslav.Shaposhnyk,
Alessandro.Villa}@ujf-grenoble.fr
<http://www.neuroheuristic.org/>

² Departament de Física i Enginyeria Nuclear
Universitat Politècnica de Catalunya, Terrassa, Spain
Javier.Iglesias@upc.edu
<http://www-fen.upc.es/>

Abstract. A scalable hardware platform made of custom reconfigurable devices endowed with bio-inspired ontogenetic and epigenetic features is configured to run an artificial neural network with developmental and evolvable capabilities. The hardware architecture allows internet-network communication and this study analyzes the simulated activity of two hierarchically organized spiking neural networks. The main features were an initial developmental phase characterized by cell death (apoptosis driven by excessive firing rate), followed by spike timing dependent synaptic plasticity in presence of background noise. The emergence of precise firing sequences formed by recurrent patterns of spike intervals above chance levels suggested the build-up of a connectivity, out of initially randomly connected networks, able to sustain temporal information processing. The relative frequency of precise firing sequences was higher in the downstream network and their dynamics suggested the emergence of an unsupervised hierarchical activity-driven connectivity.

1 Introduction

The simulation of a human artifact of ontogenetic and epigenetic processes that occur in the embryonic nervous system is a long-standing objective of the bio-inspired and evolvable hardware community. The simulation of large-scale complex systems is a core task in the framework of Perplexus, an international project aimed to develop a scalable hardware platform made of custom reconfigurable devices endowed with bio-inspired features (Sanchez et al., 2007). However, the Perplexus project is not aimed at implementing a whole model of the brain, neither of the cerebral cortex in its entirety, rather a bio-inspired neural network with developmental and evolvable capabilities.

The embryonic nervous system is initially driven by genetic programs that control neural stem cell proliferation, differentiation and migration through the

actions of a limited set of trophic factors and guidance cues (Oppenheim, 1981; Innocenti, 1995). The outcome of this phase is a pattern of neuronal connectivity characterized by a large amount of diffusely distributed branches and synapses. After a relatively short period of stable synaptic density, a pruning process begins: synapses are constantly removed, yielding a marked decrease in synaptic density (Innocenti and Price, 2005). The refinement of the nervous system in the cerebral cortex is likely to be associated with a gradient-like organization of patterns of gene expressions driving apoptosis—genetically programmed cell death—and selective axon pruning driven by synaptic plasticity (Elston, 2002; Innocenti and Price, 2005; Low and Cheng, 2006; Yamamori and Rockland, 2006). Eventually, in the adult brain the cerebral cortex is formed by a vast amount of hierarchically organized areas that can be very schematically considered as “primary” or “input” areas (if receiving a direct input from the ascending sensory pathway) “secondary” or “associative” areas (if receiving inputs from the primary areas), and “motor” or “output” areas (if projecting to the efferent system).

Synapses can change their strength in response to the activity of both pre-, and post-synaptic cells (Roberts and Bell, 2002) following spike timing dependent plasticity rules that were already successfully implemented in bio-inspired evolvable hardware (Moreno et al., 2005; Moreno et al., 2006). Certain pathways through the network may be favored by preferred synaptic interactions between the neural elements as a consequence of developmental and learning processes (Braitenberg and Schuez, 1998). In cell assemblies interconnected in this way some ordered and precise—in the order of few *ms*—interspike interval relationships, referred to as “spatio-temporal firing patterns” or “precise firing sequences”, may recur within spike trains of individual neurons and across spike trains recorded from different neurons (Abeles, 1991). It is expected that the same temporal pattern of firing would be observed whenever the same information is presented in a particular cell assembly (Villa et al., 1999; Villa, 2000). Then, firing patterns are determined by both developmental events (ontogenetic) and synaptic plasticity (epigenetic). The dynamics of firing patterns in the various cortical areas are likely to vary with the functional roles played by the areas themselves in a way to let emerge higher cognitive activities that require feature binding and compositionality (Singer, 1999; Abeles et al., 2004).

A novel and flexible hardware architecture called *ubidule* has been developed in the framework of the Perplexus project to simulate neural networks with ontogenetic and epigenetic features (Upegui et al., 2007). The present study is aimed to investigate how the dynamics of firing patterns varies in evolvable hierarchically organized neural networks. A better knowledge of these dynamics is essential for understanding how to implement the emerging cognitive properties of these networks in a multiple *ubidules* autonomous robot. The networks are organized such that selected units of the first network—assumed to correspond to its output layer—drive the input activity of the second network. The upstream network is the only one receiving an external input, thus corresponding to a “primary area”, and the downstream network corresponds to a “secondary area”. The output spike trains of both networks were scanned to detect precise firing

sequences. The structure and dynamics of the detected precise firing sequences were analyzed and compared with the results obtained for the single simulated networks in presence and in absence of stimuli (Iglesias et al., 2007).

2 Neural Network Simulations

Each network is a 2D lattice of 100 x 100 units—80% of excitatory units (*exc*) and 20% of inhibitory (*inh*) units—uniformly distributed over the network according to a space-filling quasi-random Sobol distribution (Press et al., 1992). The probability that, within each network, a unit be connected to another one followed a Gaussian density function with different parameters for excitatory and inhibitory units (Iglesias et al., 2005). All units were simulated by leaky integrate-and-fire neuromimes (Iglesias and Villa, 2007).

Background activity was used to simulate the effect of afferences that were not explicitly simulated within a network. To this end we assumed that all units received the same number of external inputs and that all of these were excitatory. Both apoptosis and synaptic pruning were taken into account in presence of a background noise (Iglesias and Villa, 2007). Apoptosis was active only at the begin of each simulation run; in this study apoptosis was active during the initial 700 *ms*. Synaptic plasticity was active from the end of apoptosis until the end of simulation.

It is assumed *a priori* that modifiable synapses were characterized by activation levels with 4 attractor states (Iglesias et al., 2005). The activation levels could be interpreted as a combination of two factors: the number of synaptic *boutons* between the pre- and post-synaptic units and the changes in synaptic conductance. In the current study we attributed a fixed activation level (meaning no synaptic modification) $A_{ji}(t) = 1$, to (*inh*, *exc*) and (*inh*, *inh*) synapses while activation levels were allowed to take one of $A_{ji}(t) = \{0, 1, 2, 4\}$ for (*exc*, *exc*) and (*exc*, *inh*), $A_{ji}(t) = 0$ meaning that the projection was permanently pruned out. For $A_{ji}(t) = 1$, the post-synaptic potentials were set to 0.84 *mV* and −0.8 *mV* for excitatory and inhibitory units, respectively. The projections from and to “dead” units undergo a decay of their synapses leading eventually to their pruning when $A_{ji}(t) = 0$. Other projections may be pruned due to synaptic depression driven by STDP and also leading to $A_{ji}(t) = 0$. Thus, some units that survived the early phase can also remain without any excitatory input. Besides cell death and axonal pruning of dead cells provoked by apoptosis, the loss of all excitatory inputs due to synaptic plasticity provoked also the cell death (even in presence of background activity) immediately after the pruning of the last excitatory afference from within the network.

In each network two sets of 400 *exc* units (*i.e.*, 800 units overall) were randomly selected among the 8,000 *exc* units. These units corresponded to the “input layer” of the network, meaning that in addition to sending and receiving connections from within the network units of both types (*exc* and *inh*) they received an external input (Fig.1a).

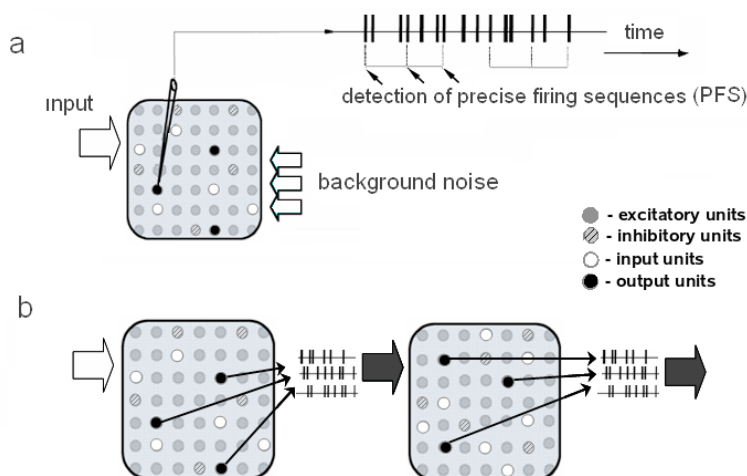


Fig. 1. Neural network diagram. **(a):** Single network diagram. The network input layer selected randomly is receiving an external input. The output layer is defined as all units having at least 5 active connections by the end of simulation. The spike trains of the output units is the network output. The spike trains are scanned for precise firing sequences (PFS). **(b):** Coupled networks. The upstream network (on the left) receives an external input and its output layer projects to the input layer of the downstream network (on the right).

An external input—the “stimulus”—was periodically fed to the input layer at the rate of 0.5 Hz . The duration of each input was 100 ms . At $t = 1\text{ ms}$ of the input 40 units out of the 400 *exc* units of the first set were randomly selected to receive a strong depolarization. At $t = 2\text{ ms}$ a depolarization was sent to another subset of 40 randomly selected units among the remaining 360 of the first set, and so on until all 400 units received a depolarization. This depolarization sequence was repeated 5 times during the first 50 ms of the input. During the following 50 ms the same procedure was applied to the second set of 400 units. Two networks were studied here. The network receiving an external input akin of sensory afferent activity was called the “upstream network”. The network receiving only an input from the upstream network was called the “downstream network” (Fig.1b). In the upstream network a subset of excitatory units not belonging to the input layer was selected as “output layer”. The output layer was formed by all units maintaining at least five active excitatory input connections from within the network after a simulation run lasting 100.000 ms with time resolution of 1 ms . The amount of units belonging to the output layer was in the range 100-150, depending on the random number generator initialization. Notice that the connections between the output layer of the upstream network and the input layer of the downstream network are synaptic connections with the activation level invariant throughout the simulation and with synaptic strengths identical to the afferent sensory projections.

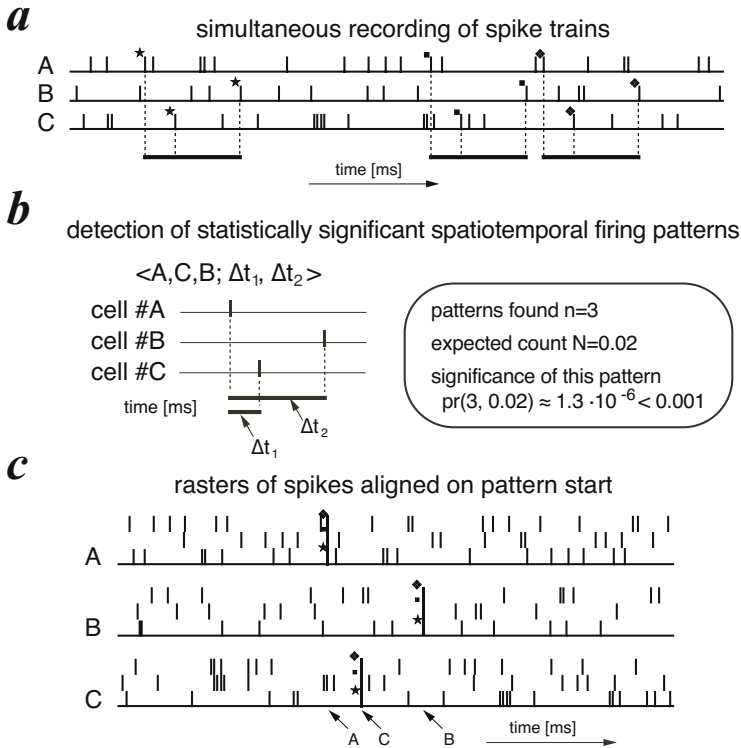


Fig. 2. Outline of the general procedure followed by pattern detection algorithms. (a): Analysis of a set of simultaneously recorded spike trains. Three cells, labeled A, B, and C, participate to a patterned activity. Three occurrences of a precise pattern are detected. Each occurrence of the pattern has been labeled by a specific marker in order to help the reader to identify the corresponding spikes. (b): Estimation of the statistical significance of the detected pattern. (c): Display of pattern occurrences as a raster plot aligned on the pattern start.

The spike trains of neuromimes of the output layer of the downstream network were recorded and searched for precise firing sequences (PFS) by means of the “pattern grouping algorithm” (PGA) (Tetko and Villa, 2001). PFS were defined as sequences of intervals with high temporal precision between at least 3 spikes (triplets) of the same or different units that recurred at levels above those expected by chance (Fig.2). PFS can be formed by spikes generated by one unit only. In this case PFS are referred to as ‘single-unit patterns’. PFS that include spikes generated by different units are referred to as ‘multi-unit patterns’. For the present study PGA was set to find patterns formed by three (triplets) or four spikes (quadruplets), with a significance level $p = 0.10$, provided the entire pattern did not last more than 800 ms and was repeated with a jitter accuracy of ± 5 ms. The current implementation of PGA allows the simultaneous analysis of only 20 spike trains. Then, the output layer was randomly subdivided into

groups of 20 units. This procedure underestimates the real number of 'multi-unit patterns' but the bias is the same and does not affect the comparison of coupled *vs.* non coupled networks.

3 Recording Conditions

For each network we recorded separately the spike trains due to the effects of background noise only. These recordings corresponded to a "control condition" necessary to evaluate the "effective spike trains" that represent the genuine activity due to network dynamics (Hill and Villa, 1997). All PFS were searched in the effective spike trains. We distinguish four recording conditions labeled 'stim OFF', 'stim ON', 'coupled 1' and 'coupled 2'.

'stim OFF': The activity of a single network was recorded in the absence of any external input and in presence of the background noise only. The effective spike trains represented the net effect of internal network dynamics shaped by spontaneous synaptic pruning.

'stim ON': The activity of the upstream network was recorded in presence of an external input corresponding to a spatiotemporal pattern of activity (Iglesias and Villa, 2007).

'coupled 1': The activity of the downstream network was recorded in presence of an external input fed to the upstream network. The pattern of connectivity between the two networks was such that each unit of the upstream output layer was connected to only one unit of the downstream input layer, randomly selected among the predefined 800 input units.

'coupled 2': The activity of the downstream network was recorded in presence of an external input fed to the upstream network. The pattern of connectivity between the two networks was such that the upstream output layer was characterized by divergent projections onto the downstream input layer. Each of the 800 units of the downstream input layer were receiving a projection from one unit of the upstream output layer.

4 Results

Precise firing sequences are simply referred below as "patterns". Because of a high sensitivity to the initial conditions we repeated all simulation runs with 30 different random generator seeds. Table 1 shows cumulated statistics over all 30 simulation runs. This Table shows that in absence of an external input ('stim OFF') more units survive at the end of the simulation run. In case of coupled networks more patterns were found in proportion to the number of active cells. Moreover, in coupled networks each pattern tended to appear more often.

It is important to notice that both 'stim ON' and 'coupled 2' networks were characterized by 800 external afferent inputs. Despite this similarity there is a decrease in about 10% of the amount of surviving cells in the 'coupled 2' network

Table 1. Patterns statistics summarized for 30 simulation of each series: numbers of active cells by the end of simulations; number of Detected Patterns with 'Active Cells- Detected Patterns' ratio in parentheses, number of occurrences of detected precise firing sequences with average number of occurrences per pattern in parentheses; 'Triplet/Quadruplet' ratio; number of detected multi-unit patterns

	stim OFF	stim ON	coupled 1	coupled 2
Active Cells				
<i>total</i>	5352	4240	4860	3763
<i>per simulation</i>	178 ± 35	141 ± 33	192 ± 41	125 ± 44
Detected Patterns				
<i>total</i>	97 (3.7%)	147 (3.5%)	241 (5%)	168 (5%)
<i>per simulation</i>	3.2 ± 3.3	4.9 ± 3.0	8.0 ± 3.6	5.6 ± 4.1
Pattern Occurences				
<i>total</i>	7359 (38.5)	5672 (37.4)	9373 (39.9)	7853 (46.8)
<i>per simulation</i>	245 ± 128	189 ± 152	312 ± 166	292 ± 171
Triplets/Quadruplets	59/138=0.4	54/93=0.6	107/134=0.8	89/99=0.9
Multi-unit Patterns	6	5	8	12

by the end of simulation. The ratio of detected patterns vs. active cells was close to 5% in the downstream network and $< 4\%$ in the upstream network (Table 1, second line). This difference seems small overall but it was significant by χ^2 -test ($p < 0.05$). The PGA algorithm detected all repetitions of the same precise firing sequence in the spike trains. Notice that the average number of repetitions per pattern increased in the downstream network (up to 46.8 in 'coupled 2').

In all recording conditions we observed more patterns formed by four spikes (quadruplets) vs. patterns formed by three spikes (triplets). However, the ratio of triplets over quadruplets tended to become closer to 1 in coupled networks (Table 1, third line). In principle one could expect that most triplets corresponding to subpatterns of a significant quadruplet would also be counted among the significant triplets. This is generally not the case because of the very stringent tests of significance carried on triplets that bias the pattern detection in the sense of underestimating the number of triplets (Tetko and Villa, 2001). Most patterns were single-unit patterns but generally the units that were involved were different from pattern to pattern. Depending on the recording condition we observed only 1–3 units that produced more than one single-unit pattern. Multi-unit patterns were observed in all networks and they were more frequent in the 'coupled 2' downstream network. The probability of multi-unit pattern detection is very small due to the PGA sampling procedure for selection of the spike trains to be analyzed simultaneously. Then, the increase in frequency of multi-unit patterns could not be assessed with reliable confidence.

The internal temporal structure of precise firing sequences was further investigated. The analysis of the distribution of the intervals between the events forming the patterns was performed with the triplets by separating the intervals between the first and second events of the pattern (Fig. 3a,c,e,g) and the intervals between the second and third events of the pattern (Fig. 3b,d,f,h). In

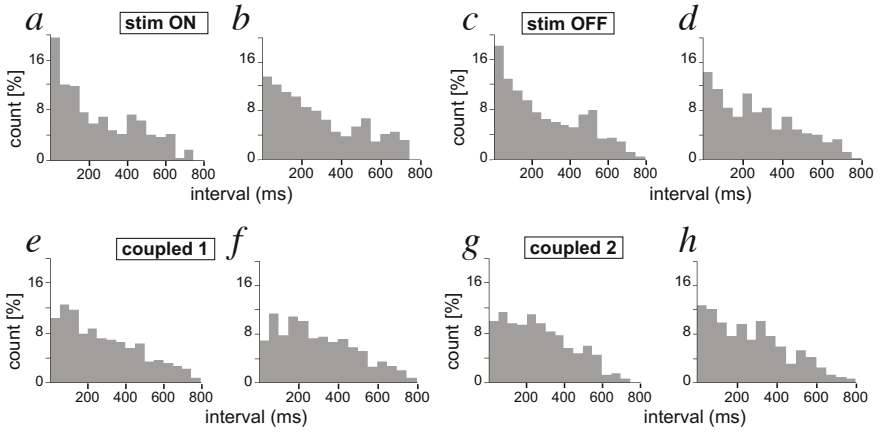


Fig. 3. Distribution (relative frequency) of the intrapattern intervals for triplets. Bin size: 50 *ms*. (**a,c,e,g**): first interval (between the first and second spike of the pattern). (**b,d,f,h**): second interval (between the second and third spike of the pattern).

case of quadruplets, for this analysis we considered the triplets corresponding to the subpatterns. The temporal structure of patterns tended to be different in the downstream network as indicated by the decrease of short first intervals

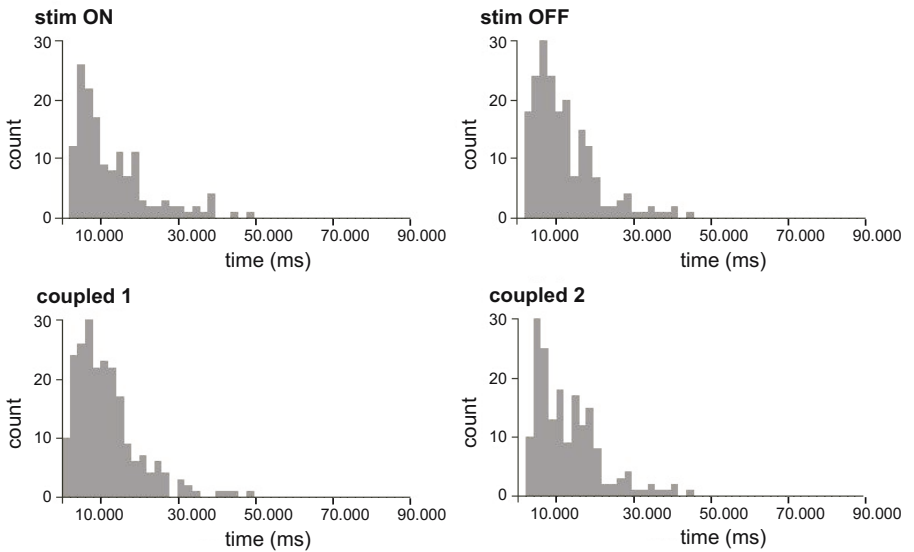


Fig. 4. Histogram of the onset time of all patterns. Bin size: 2000 *ms*. Notice the shift of the distribution towards later times for 'coupled 1' and 'coupled 2' networks, but in all cases the patterns appeared before time $t = 50.000$ *ms*.

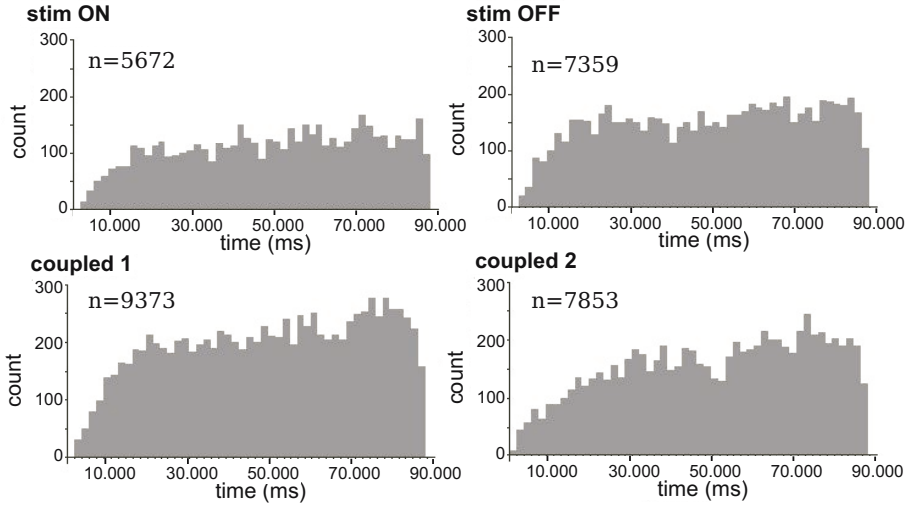


Fig. 5. Distribution of the epochs of all events belonging to all patterns. Bin size: 2000 ms. Notice the less steep slope for the 'coupled 2' downstream network.

(Fig. 3e,g) compared to the first intervals of the upstream network in presence (Fig. 3a) and in absence of stimulation (Fig. 3c) as well.

Figure 4 shows the distribution of the onset time of the first occurrence of each pattern. In all recording conditions most patterns appeared before $t = 30.000\text{ ms}$ and not later than $t = 50.000\text{ ms}$. In the downstream network (in particular 'coupled 2') the patterns tended to appear later during the simulation. Figure 5 shows the distribution of the epochs of all spikes belonging to all repeated patterns. It is interesting to notice that after a certain delay the probability to find a spike belonging to a pattern tended to be almost constant for all recording conditions. However, such *plateau* was reached much later for the most interconnected downstream network (Fig. 5 'coupled 2'), at a time near $t = 35.000\text{ ms}$.

5 Discussion

The present study analyzes the activity dynamics of two interconnected neural networks that are hierarchically connected with respect to an external stimulus. The hardware compatible simulation was designed in order to be implemented on a scalable hardware platform (Sanchez et al., 2007) retaining much of the biological neural development features (*i.e.*, spiking neural networks characterized by a brief initial phase of cell death followed by STDP and synaptic pruning) (Innocenti and Price, 2005). The custom designed *ubidule* hardware is currently tested and a hardware implementation of the experiment presented here is scheduled in the year 2009.

It is foreseen that the hardware implementation of a spiking neural network on an *ubidule* will allow simulation and study of more complex hierarchical organizations including a larger number of neural networks exchanging their neural activity. This exchange will be based on the sensory (“input layer”) and actuator (“input layer”) units provided that each *ubidule* is equipped with an encoder and a decoder able to transmit the activity of the neural network over the wireless network that it used for inter-*ubidules* communication. The input layer of a network can be wired to receive inputs from either a hardware sensor (photodiode, camera, microphone, mechano-sensor, . . .), thus representing the upstream network of this study, or from other *ubidules*, thus representing the downstream network. The actuator units could also be wired to hardware actuators (diode array, loudspeaker, electrical motor, . . .) and/or to an encoder broadcasting their activity over the wireless network.

The present results show that the downstream network activity was characterized by fewer surviving units at the end of the simulation run. This difference was only due to synaptic pruning driven by spike timing dependent plasticity because cell death provoked by apoptosis was similar for both upstream and downstream networks. In presence of the external stimulus PFS observed in the upstream network were relatively more frequent than in the absence of stimulation, in accordance with results presented elsewhere (Iglesias and Villa, 2007). The analysis of the onset time of the patterns and their internal dynamics suggests that downstream networks took more time to build-up the connectivity underlying the emergence of the patterns. The finding of what could be viewed as an increase in “complexity” of the temporally organized activity in the downstream network was achieved with less active units and in a totally unsupervised way. These results suggest that precise firing sequences might be the most relevant information to be transmitted by *ubidules* in an open-field arena. Information processing carried by such patterned activity (Abeles et al., 2004) was suggested to play a key-role in achieving compositionality of mental representations (Fodor and Pylyshyn, 1988).

Acknowledgments. This work was partially funded by the European Union New and Emerging Science and Technology Complex Systems program grant #034632 (PERPLEXUS) and NEST program grant #043309 (GABA) and the Swiss National Science Foundation SNF grant #PA002-115330/1.

References

- Abeles, M.: *Corticonics: Neural Circuits of the Cerebral Cortex*, 1st edn. Cambridge University Press, Cambridge (1991)
- Abeles, M., Hayon, G., Lehmann, D.: Modeling compositionality by dynamic binding of synfire chains. *Journal of Computational Neuroscience* 17, 179–201 (2004)
- Braitenberg, V., Schuez, A.: *Cortex: statistics and geometry of neuronal connectivity*, 2nd edn. Springer, Berlin (1998)
- Elston, G.N.: Cortical heterogeneity: implications for visual processing and polysensory integration. *J. Neurocytol.* 31, 317–335 (2002)

- Fodor, J., Pylyshyn, Z.: Connectionism and cognitive architecture: A critique. *Cognition* 28, 3–71 (1988)
- Hill, S., Villa, A.E.: Dynamic transitions in global network activity influenced by the balance of excitation and inhibition. *Network: computational neural networks* 8, 165–184 (1997)
- Iglesias, J., Chibirova, O., Villa, A.: Nonlinear dynamics emerging in large scale neural networks with ontogenetic and epigenetic processes. In: de Sá, J.M., Alexandre, L.A., Duch, W., Mandic, D.P. (eds.) *ICANN 2007. LNCS*, vol. 4668, pp. 579–588. Springer, Heidelberg (2007)
- Iglesias, J., Eriksson, J., Grize, F., Tomassini, M., Villa, A.E.: Dynamics of pruning in simulated large-scale spiking neural networks. *BioSystems* 79(1), 11–20 (2005)
- Iglesias, J., Villa, A.E.P.: Effect of stimulus-driven pruning on the detection of spatiotemporal patterns of activity in large neural networks. *BioSystems* 89, 287–293 (2007)
- Innocenti, G.M.: Exuberant development of connections, and its possible permissive role in cortical evolution. *Trends in Neurosciences* 18(9), 397–402 (1995)
- Innocenti, G.M., Price, D.J.: Exuberance in the development of cortical networks. *Nature Reviews Neuroscience* 6, 955–965 (2005)
- Low, L.K., Cheng, H.-J.: Axon pruning: an essential step underlying the developmental plasticity of neuronal connections. *Philosophical Transactions of the Royal Society* 361(1473), 1531–1544 (2006)
- Moreno, J.M., Eriksson, J.L., Iglesias, J., Villa, A.E.: Implementation of biologically plausible spiking neural networks models on the POETic tissue. In: Moreno, J.M., Madrenas, J., Cosp, J. (eds.) *ICES 2005. LNCS*, vol. 3637, pp. 188–197. Springer, Heidelberg (2005)
- Moreno, J.M., Thoma, Y., Sanchez, E., Eriksson, J., Villa, A.E.P.: The poetic electronic tissue and its role in the emulation of large-scale biologically inspired spiking neural networks. *Complexus* 3, 32–47 (2006)
- Oppenheim, R.W.: Studies in developmental neurobiology: essays in honor of viktor hamberger. In: Cowan, W.M. (ed.) *The neurotrophic theory and naturally occurring motoneuron death*, Oxford University Press, New York (1981)
- Press, W.H., Flannery, B.P., Teukolsky, S.A., Vetterling, W.T.: Numerical recipes in C: The art of scientific computing, 2nd edn. Cambridge University Press, Cambridge (1992), <http://www.nr.com/>
- Roberts, P.D., Bell, C.C.: Spike timing dependent synaptic plasticity in biological systems. *Biol. Cybern.* 87, 392–403 (2002)
- Sanchez, E., Perez-Urbe, A., Upegui, A., Thoma, Y., Moreno, J.M., Villa, A., Volken, H., Napieralski, A., Sassatelli, G., Lavarec, E.: Perplexus: Pervasive computing framework for modeling complex virtually-unbounded systems. In: *AHS 2007: Proceedings of the Second NASA/ESA Conference on Adaptive Hardware and Systems*, pp. 587–591. IEEE Computer Society, Washington (2007)
- Singer, W.: Neuronal synchrony: a versatile code for the definition of relations? *Neuron* 24, 49–65 (1999)
- Tetko, I.V., Villa, A.E.: A pattern grouping algorithm for analysis of spatiotemporal patterns in neuronal spike trains. 1. detection of repeated patterns. *Journal of Neuroscience Methods* 105, 1–14 (2001)
- Upegui, A., Thoma, Y., Sanchez, E., Perez-Urbe, A., Moreno, J.M., Madrenas, J.: The perplexus bio-inspired reconfigurable circuit. In: *AHS 2007: Proceedings of the Second NASA/ESA Conference on Adaptive Hardware and Systems*, pp. 600–605. IEEE Computer Society, Washington (2007)

- Villa, A.E.P.: Empirical evidence about temporal structure in multi-unit recordings. In: Miller, R. (ed.) *Time and the Brain*, ch.1, pp. 1–51. Harwood Academic Publishers (2000)
- Villa, A.E., Tetko, I., Hyland, B., Najem, A.: Spatiotemporal activity patterns of rat cortical neurons predict responses in a conditioned task. *Proc. Natl. Acad. Sci. USA* 96, 1106–1111 (1999)
- Yamamori, T., Rockland, K.S.: Neocortical areas, layers, connections, and gene expression. *Neurosci. Res.* 55, 11–27 (2006)